A R C H I V E S O F M E T A L L U R G Y A N D M A T E R I A L S
Volume 50 2005 Issue 1

J. HIRSCH*

TEKSTURE AND ANISOTROPY IN INDUSTRIAL APPLICATIONS OF ALUMINIUM ALLOYS[1)]

TEKSTURA I ANIZOTROPIA W PRZEMYSŁOWYCH ZASTOSOWANIACH STOPÓW ALUMINIUM

Texture and anisotropy in industrial processed Aluminium alloys and some typical Aluminium products are presented. The main texture components observed in ascast, deformed and annealed (recrystallized) aluminium are described and discussed together with the principles of their formation mechanisms. Typical examples are given for texture effects on resulting properties and anisotropy, like strength and formability effects in Al-Mg-Si alloys for can body and automotive sheet applications, or for age hardening variations in different sections of Al-Li extrusions and for etching behaviour of 100 μ high purity Aluminium capacitor foil.

W pracy przedstawiono tekstury i anizotropię w stopach aluminium poddanych procesom technologicznym jak też w kilku typowych wyrobach aluminiowych. Zostały opisane główne składowe tekstury obserwowane w materiale po odlaniu, po deformacji i po rekrystalizującum wyżarzaniu. Przedstawiano dyskusję na temat mechanizmy formowania się tych składowych. Podano typowe przykłady wpływu tekstury na właściwości i anizotropię materiału, jak na wytrzymałość i odkształcalno w stopach Al-Mg-Mn and in Al-Mg-Si do produkcji puszek i blach samochodowych, lub na zmiany utwardzania wydzieleniowego w różnych przekrojach wyciskanego stopu Al-Li jak też na zachowanie się w czasie trawienia folii kondensatorowej o grubości 100 μm z aluminium o wysokiej czystości.

1. Introduction

Industrially processed Aluminium alloys often show strong crystallographic textures, some of which unintended, but in many cases they are induced intentionally — or

* HYDRO ALUMINIUM DEUTSCHLAND GMBH, R&D, BONN, GERMANY
1) invited lecture

at least controlled — due to a strong — sometimes beneficial impact on specific properties, i.e. anisotropy [1-3]. Due to an ever-increasing demand for best material quality and optimum performance the control of this microstructure feature is gaining more and more importance. It can now be more thoroughly investigated and analyzed due to major progress in measuring techniques (e.g. automatic X-ray diffraction goniometers or REM with EBSD equipment) and evaluation methods [4– 9].

Since new measuring techniques are being implemented in industrial R&D, some important progress has been achieved and systematic knowledge accumulated. Texture control during industrial processing, like rolling, annealing and extrusion of Al-alloys is now possible and applied due to available data acquisition and visualization software and due to a better understanding on the basis of a scientifically sound interpretation of the underlying mechanisms.

For standard processed Aluminium, like sheet or extrusions, texture evolution and anisotropy effects can be described by a relative small number of characteristic texture components. These form due to an oriented growth selection during solidification, the restriction of crystallographic slip during deformation or due to nucleation and growth selection during recrystallization annealing. The principle mechanisms have often been described and analyzed using advanced experimental and characterization methods and their effects on material properties like strength, formability and surface effects (e.g. [10-15]). In the following the main characteristic textures that occur in different processes of Aluminium semi fabrication and processing are described and the principle effects on characteristic variations in strength, formability and chemical etching will be discussed.

2. Texture effects in the main steps of material processing

2.1. Solidification textures

During solidification commercial Aluminium alloys mostly form random textures due to heterogeneous nucleation when fast cooling and grain refinement is applied [16,17] (Fig. 1a).

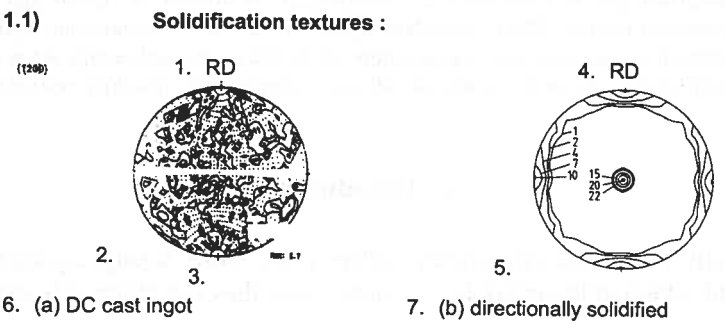

Fig. 1. (a) Random and (b) <100> fiber texture of cast pure aluminium

However, when uni-directional solidification occurs e.g. under different (local) cooling conditions a preferred crystallographic < 100 > fibre texture can be generated [8], as shown in Fig. 1b. In some of these cases even solidification twinning may occur in Aluminium that produces the typical solidification structure of "feathery" crystals, showing a preferred < 112 >-fiber axis due to its specific low energy configuration.

2.2. Deformation textures

For any equiaxed, uni-directional deformation like wire drawing or equiaxial tension or extrusion the texture formation consists of an alignment of preferred crystallographic axes in the major deformation (e.g. extrusion) direction. Here a typical double fiber with varying < 111 > and < 100 > fiber components is formed (Fig. 2a). During uniaxial compression and equiaxed forging, in contrast, the < 110 > direction is the stable orientation and thus the observed (preferred) fiber texture component [20].

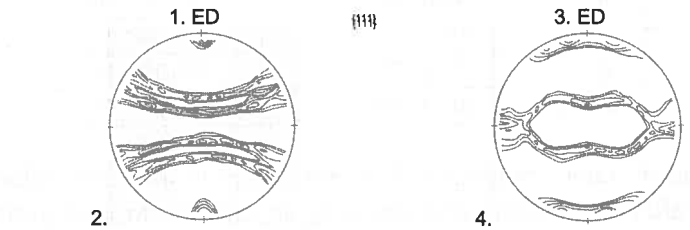

Fig. 2. (a) Fiber type and (b) plane strain (rolling-type) textures of extruded Al-Li (8090) alloy in two sections of the same profile formed in a locally different plane strain (flat) and uniaxial (square) deformation geometry (ED = extrusion direction) {111} pole figures

During plane strain compression deformation like sheet rolling or flat profile extrusion the typical ("plane strain") rolling texture is observed [3.9] (Fig. 2b) with the main components listed in table 1a. It mainly consists of a series of orientations oriented aligned along the "β-fiber" which can be described by a ± 35° rotation around a < 110 > axis that lies tilted 60° from the normal direction, ND, towards the rolling direction, RD [9].

2.3. Recrystallization textures

The corresponding typical recrystallization texture components of rolled (plane strain deformed) and annealed aluminum sheet alloys are listed in table 1 b) [9,10]. The two most prominent ones (cube and R) are easy to detect in conventional pole figure analysis (Fig. 3a). They can be related to specific recrystallization mechanisms (see below, [10-12]). Others are less obvious or weaker and have only recently been identified and analyzed by systematic and more detailed texture investigations using

advanced texture measurement and evaluation methods, e.g. 3-dimensional ODF or EBSD [6, 13] (Fig. 3b).

TABLE

Main plane strain deformation (rolling) and corresponding recrystallization texture components in Aluminum alloys

Name	Miller indices {hkl} <*uvw*>	Euler angles $\varphi_1, \Phi, \varphi_2$
a) plane strain (rolling) deformation texture components		
C	{112}<111>	90°, 35°, 45°
S	{124}<211>	63°, 31°, 60°
B	{011}<211>	35°, 45°, 0°
b) corresponding recrystallization texture components		
Cube	{001}<100>	0°, 0°, 0°
R	{124}<211>	63°, 31°, 60°
P	{011}<122>	70°, 45°, 0°
Q	{013}<231>	45°, 15°, 10°
Goss	{011}<100>	0°, 45°, 0°

The 'classical' cube component (Fig. 3a) occurs in most hot rolled and annealed Al- alloys or after cold rolling and annealing in medium to high purity Aluminium. It also occurs in age hardening alloys, here sometimes with characteristic shifts or scatterings (see below and [13]). The R component (Fig. 3a) is very similar to the

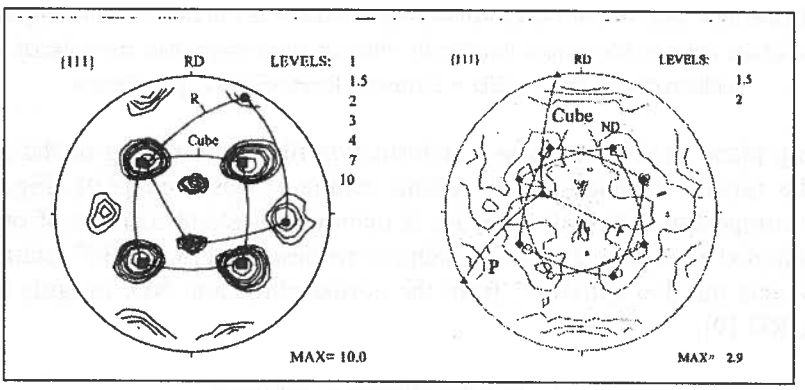

Fig. 3. Typical recrystallization textures of rolled Aluminium Alloys
a) Cube and R texture in 95% rolled commercial purity Aluminium (AA1145),
b) ND rotated Cube and P texture in age hardenable Al.-Mg-Si (AA6111)

main S rolling texture component [9] indicating either an in-situ recrystallization or strain induced boundary migration (SIBM) nucleation process with subsequent growth [12]. The so-called "P" component (Fig. 3b, "P" originates from "PSN" — explanation

see chapter 3.2 below), and the "Q" component (a component close to the rotated cube texture, not shown here) originates at deformation inhomogeneities, i.e. particles or shear bands [12, 13].

3. Textures in industrial aluminium production

3.1. Texture evolution during hot rolling

Fig. 4 illustrates the typical processing route of aluminum alloy sheet production. The starting material is a conventional DC-cast ingot, which contain a typical cell structure with the grain formation usually controlled by grain refinement, therefore having a mostly random texture (Fig. 5a). For the hot rolling, the ingots are preheat-

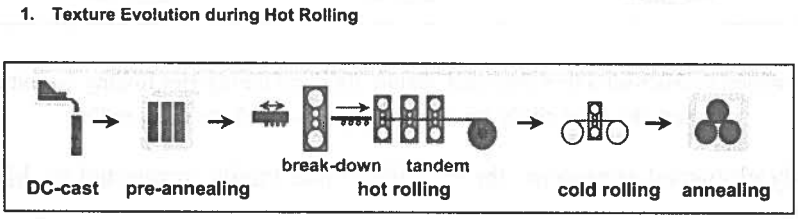

Fig. 4. Typical processing steps for Al-alloy sheets

ed to a temperature between 450°C and 600°C where the material is homogenized, short-range intercellular segregations (coring) are removed and soluble phases in the material are dissolved [3, 16]. During hot rolling operations of thick slab material (from about 600 mm down to 3 to 12 mm hot line gauge), concurrent deformation and recrystallization occur having a strong impact on the overall microstructure and texture evolution (Fig. 5b,c). Here the formation of cube texture is typical for all aluminum alloys that recrystallize during or after hot rolling by additional hot strip annealing.

Any industrial sheet production equipment is optimized for maximum mass output. Multi-stand hot rolling lines are most efficient due to their significant advantages in high speed, short inter-pass times maintaining high temperatures and high reduction steps. This also implies fast and easy recrystallization, e.g. directly out of the rolling heat without additional reheating, referred to as "self annealing". Therefore, compared to reversing hot rolling lines, the tandem hot rolling parameters involve high temperatures, strain and strain rates at short inter-stand time which can produce smaller grain sizes and a significant increase in cube texture [16] (Fig. 5c).

The origin of the cube texture is seen in preferred nucleation sites in the (hot) deformation substructure with significantly larger subgrain size, i.e. in an advanced state of recovery which enhances nucleation [10]. Additionally, subsequent consumption of other rolling texture orientations in the surrounding, less recovered substructure is ensured by its large and preferably growing misorientation. Cube nuclei develop

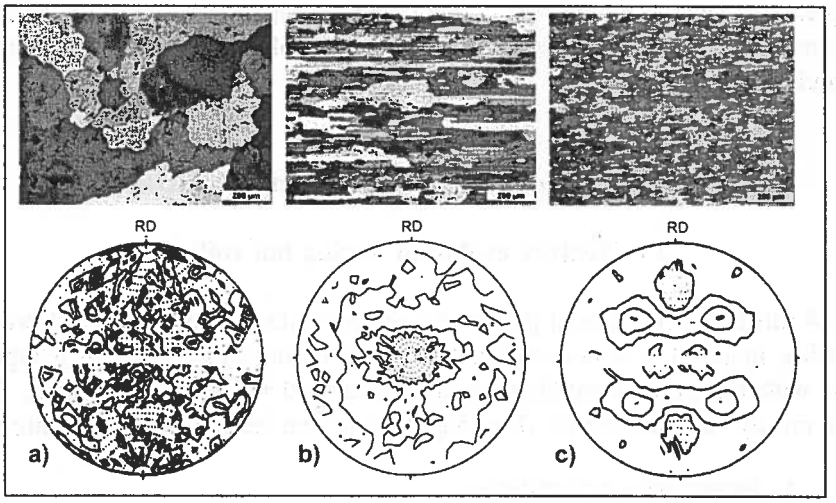

Fig. 5. Evolution of Microstructure (top) and Texture (bottom) during Hot Rolling: a) Initial as-cast structure, b) After single stand (reversing), c) Multi-stand hot rolling

from highly elongated subgrains, the so-called cube bands, supported by high rolling reductions.

Full or significant partial recrystallization in preceding rolling steps — either during hot rolling or by intermediate annealing — considerably reduces the final cube texture strength. This means that large recrystallized fractions after preceding passes reduce cube texture strength [16] while short inter-pass times (as in multi-stand hot rolling lines) or reduced temperatures are beneficial. Thus, for maximum cube texture — as necessary for can body stock — an optimum combination of hot rolling process parameters is required which is best achieved by controlled rolling schedules.

3.2. Texture evolution after cold rolling and annealing

When rolling temperatures are too low and/or high strain rates occur the cube texture decreases again since other nucleation sites become active [10]. In particular, particle stimulated nucleation ("PSN") begins to play a role, especially in commercial aluminum alloys which contain sufficiently large particles, *viz.* μm-sized constituents. PSN shows typical P and rotated cube texture components (Fig. 3b). However, it also has a strong randomizing effect and significantly reduces recrystallization texture sharpness[13]. It is very effective in highly cold rolled and annealed material in supersaturated precipitation hardening alloys of technical purity (see chapter 3.3).

While the cube orientation is the dominant hot rolling recrystallization texture component in cold rolled and annealed aluminum of commercial purity competing recrystallization mechanisms are active producing PSN (random) and R texture (a component very similar to the S rolling texture component (see Fig.3a and table 1). The cube component is dominant in high purity aluminum rolled to thin gauges (100μm) and

annealed under controlled conditions [20]. Here it can reach almost 100% volume, i.e. a virtual single crystal sheet is produced (Fig. 6a). With further cold rolling, however, it is significantly reduced due to erased cube nuclei, thus affecting final properties (e.g. for high capacity condenser foil applications, see chapter 4.4).

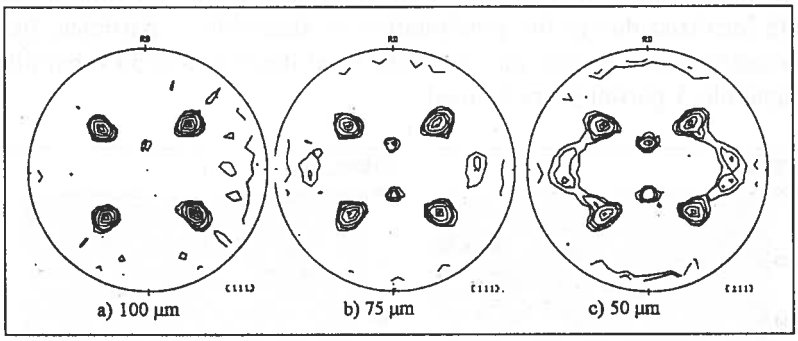

Fig. 6. {111} pole figures of highly cold rolled and annealed high purity (4N) Aluminum foil showing strong cube and R-texture variations at different finish gauges: a) 100μm, b) 75μm, c) 50μm thickness

4. Examples of texture effects on material properties

4.1. Strength variation in age hardening of extruded Al-Li Alloys

Any variation in crystallographic texture has an immediate impact on material strength due to the changes in geometry of the different slip systems activated upon ongoing or subsequent deformation. The most simple explanation for this can be given by assuming single slip only on the slip system with the highest orientation factor m ($= 1/\text{Schmid}-\text{factor}\mu = \cos\lambda * \cos\chi$, with λ and χ being the angle between tensile and slip plane normal and slip direction, respectively) in a tensile test where the variation can be up to 84% (m varies from 3.67 for the $< 111 >$ direction to 2 for a central direction with $\lambda = \chi = 45°$), neglecting any orientation dependent strain hardening effects during deformation! For the other extreme of multiple slip (a minimum of 5 slip systems) as defined by the Taylor model the variation still can be as high as 61%. Any slip system activation will occur within the limits of these two models, so the variation range in strength can be estimated accordingly.

In addition to individual orientation, the selection of slip systems also depends on any microstructural feature that affects local dislocation glide like grain boundaries, grain misorientation and particles. For the aspects of grain interaction, refined deformation texture simulation models have been formulated [9, 21]. The effect of particles, however, is much less investigated but can be quite important for precipitation strengthened Al alloys, where the effect of shearable and un-shearable particles changes the slip mechanisms, depending on age hardening. This is illustrated in the age hardening

curves of the Al-Li AA8090 material measured in two different sections of the same extrusion showing two different textures (Fig. 2 a and b) [15]. The corresponding age hardening response (Fig. 7a) for the two areas is very similar in the solution treated and over-aged condition (difference about 15%) but drastically increased (to >25%) in the under-aged condition (Fig. 7b). This difference has its maximum values when slip is quite localized due to the precipitation of shearable δ' particles. In peak- and over-aged condition it falls back on its normal level (typical also for other alloys) when the non-shearable S particles are formed.

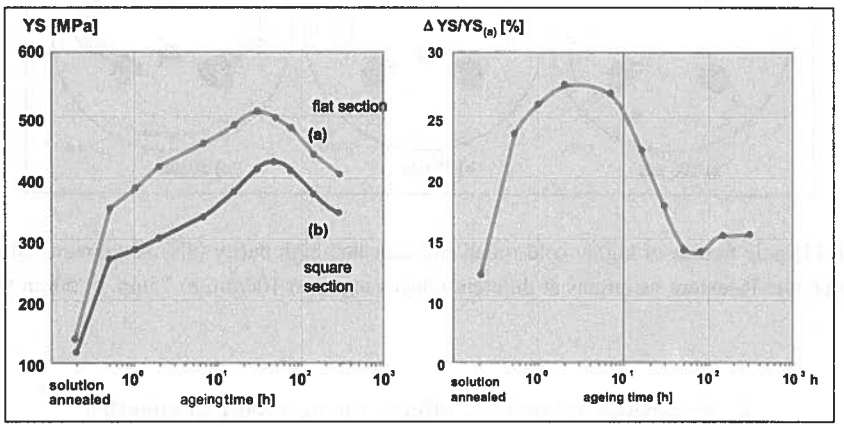

Fig. 7. Yield strength evolution during age hardening measured in a single Al-Li profile on different sections (textures see Fig. 2). a) yield strength evolution during age hardening, b) relative difference in yield strength between sections a) and b)

The corresponding orientation factor calculation reveals a small difference of only 8% in Taylor factor M for multiple slip but reaches 27% for single slip. Thus the combination of the two effects can explain the observed drastic strength difference in the two sections of the structural part (produced in a single fabrication process [15]):

i)Different local textures — due to local differences in deformation geometry during extrusion — and

ii)Different slip system activation geometry — due to changes in precipitation effects on slip.

4.2. Anisotropy effects in deep drawing of Al-Mg-Mn alloy sheet

Strong textures will cause characteristic anisotropic material flow behavior (so called "ears") when sheets are deep drawn into a cup from a circular blank, as shown in Fig. 8. The cube texture (e.g. Fig. 5c) which is typical for Aluminum alloys that recrystallize during or after hot rolling causes strong 0°/90° ears, as shown in Fig. 8b. This effect is technically quite important, e.g. for AlMg1Mn1 can body stock, where a strong hot strip cube texture is required for low earing and good formability of the

1. **Anisotropy effects in deep drawing operations of Al sheet :**

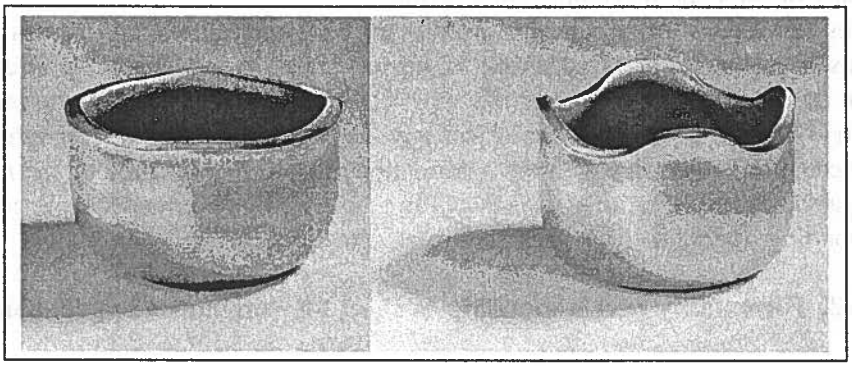

Fig. 8. Deep drawn cups from circular blanks of Al-Mg-Mn can body stock hot strip with (a) rolling and weak cube texture and (b) strong cube texture (e.g.Fig. 5c)

cold rolled finish gauge sheet [14]. While in the fully recrystallized hot strip the cube texture causes a characteristic 0°/90° anisotropy (Fig.8b = Fig.9c), subsequent cold rolling generates strong 45° ears in the 0.3 mm finish gauge sheet. This can be reduced by a strong (controlled) cube starting (i.e. hot strip) texture with 0°/90° ears (Fig.9c) [3, 16], in contrast to an unacceptable increase in 45° earing for an unrecrystallized hot strip (as in Fig. 9a).

In other cases, however, where hot strip itself is used for forming operations a more isotropic deformation behaviour in the initial condition (as in Fig. 9b) might be required, e.g. for the deep drawing of wheel disk fabricated from a 8 mm AlMg3 hot strip. Here optimum formability is provided by controlled partial recrystallization

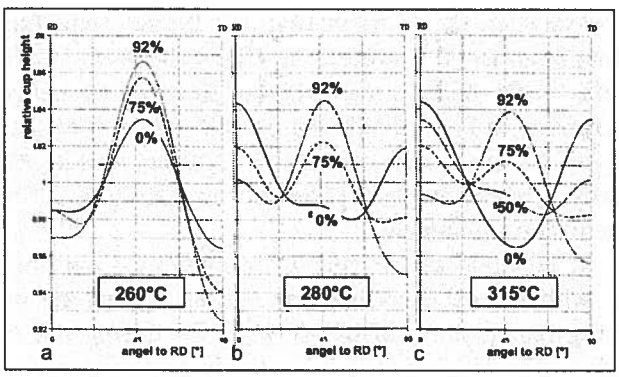

Fig. 9. Evolution of cup profiles (symmetrized, from 0° to 90°) of AlMg1Mn1 hot strip produced at different temperatures (a-c), then cold rolled from 0% (full lines) to 92% reduction

where some of the hot rolling texture is preserved to effectively balance the opposite anisotropy of the cube recrystallization texture.

Thus, an almost even cup rim profile can be produced (as e.g. shown in Fig. 8a). This is required since besides the earing response, strong anisotropy effects also occur in the thickness of the flange that may lead to severe deviations in the rotational symmetry. The required condition of isotropy can also be measured in simple tensile tests since earing correlates with the deformation anisotropy evaluated by the r- value, defined as deformation ratio: $\epsilon_{width}/\epsilon_{thickness}$ in a uni-axially deformed sample cut in the corresponding directions of a sheet (but rotated by 90°!) [13].

4.3. Formability effects in Al-Mg-Si sheet for automotive applications

As discussed above, a random orientation distribution is usually attributed to the PSN recrystallization mechanism. However, in high-resolution texture analysis weak but characteristic texture effects can clearly be observed [12]. In some cases the corresponding weak recrystallization texture (as shown e.g. in Fig. 3b) is actually very close to a complete 40° <111> transformation of the rolling texture, caused by growth selection out of the large spectrum of mostly randomly oriented nuclei growing around the particles already at incipient stages of recrystallization ('microscale growth selection') [13].

Fig. 3b shows the typical features of a recrystallization texture that is obtained in a heat-treatable AlMgSi 6xxx alloy where recrystallization is governed by PSN. In most cases, however, PSN is not the only nucleation mechanism. PSN competes with other nucleation mechanisms at other sites, in particular those of the cube texture. In such instances the final texture type and sharpness depends on the relative amounts of nucleation at either side. This is illustrated in Fig. 10 a-c where the influence of homogenization and precipitation coarsening during the initial ingot preheating treatment on the textures found in the final recrystallized sheets is revealed.

The recrystallization textures in the Al-Mg-Si alloys consist of the cube orientation with RD and/or ND scatter, the P orientation and the R orientation in all cases, i.e. for all pre-annealing treatments. However, the ODFs shown in Fig. 10 disclose further significant variations in the relative intensities of these components as well as in the overall texture sharpness. In Fig. 10 only the φ_2 = 0°-sections of the ODFs are shown, where the intensity of the exact cube orientation together with its RD- scatter are seen which systematically increase at the expense of the PSN (e.g. "P") orientations with increasing homogenization treatment.

The decrease of cubeND and P (the R orientation – not shown in Fig. 10 — appeared to scale with the cube orientation) reveals a decrease in the efficiency of PSN with increasing precipitation of Mg_2Si-particles during hot rolling and/or final annealing. As discussed in detail in [13], these finely dispersed particles tend to impede PSN more strongly than nucleation at the cube-bands. Hence, nuclei emerging from the cube-bands (i.e. cube- and cubeRD oriented grains) and the grain boundaries (i.e. R oriented grains) will prevail in the corresponding recrystallization texture [12].

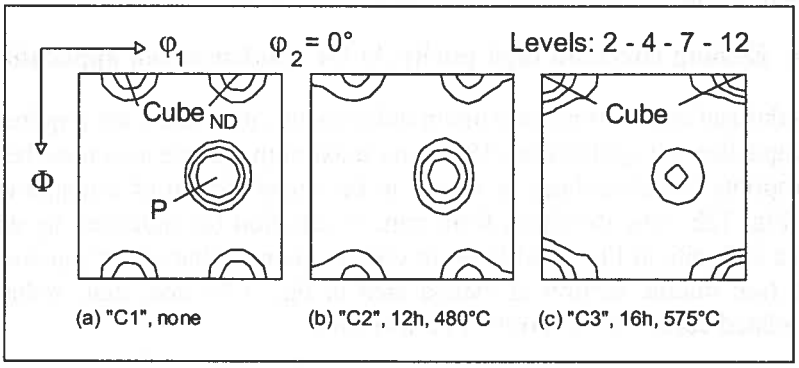

Fig. 10. Recrystallization textures in AA6010 Al-Mg-Si sheet "C" with systematic variations of cube and PSN ("P") texture components due to different ingot pre-annealings

Fig. 11 illustrates the resulting plastic anisotropy in terms of the variation in r (α) (Fig. 11a) and the (symmetrized) earing profiles h (α) of deep drawn cups (Fig. 11b) for the three different materials. Evidently, the texture variations have a strong impact on the resulting plastic anisotropy. The PSN textures with fairly strong cube_{ND} and P orientations (e.g. homogenization states C-1 and C- 2, see Fig. 10 a, b generate maxima for both earing and r-values at an angle of about 45° to the RD and minima at α = 0°/90°.

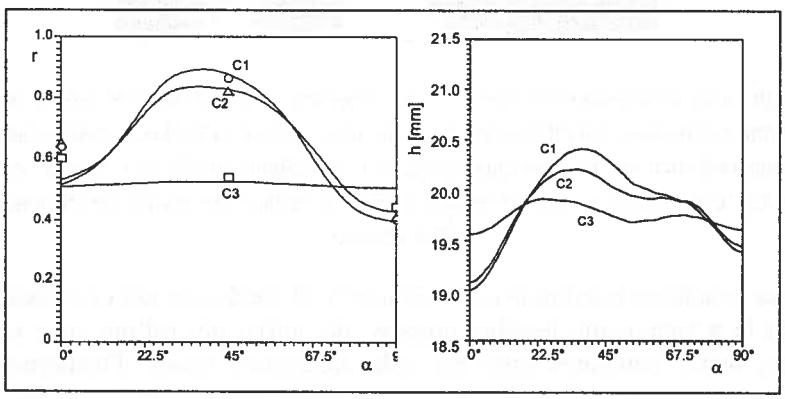

Fig. 11. Plastic anisotropy due to PSN texture variations (C1-C3, shown in Fig. 10), In form of a) r-values and b) earing profiles (C3 with the most balanced anisotropy)

Thus, texture control starts very early in the processing chain and can be applied to balance the pronounced anisotropic properties of the prevalent cube-recrystallization texture with the opposite 0°/90°-ears and minimum r-values at 45°. Here additionally theoretical r-values were computed from the texture data [21] to give the complete r

(α)-curves fitted to the experimental points in Fig. 11a. This underlines the predictable strong effect of the crystallographic texture on the plastic anisotropy.

4.4. Etching effects in high purity Al for condenser foil applications

For industrial applications maximum cube texture intensities are required for high capacity capacitor foil application /18/ where maximum surface area must be produced after appropriate tunnel etching as shown in the cross section of a tunnel etched foil shown in Fig. 12b. Any deviation from cube orientation (as indicated by white areas and surface etch pits in Fig. 12a) leads to oblique tunnels that affect penetration angle and depth (see middle section of etched area in Fig. 12b) and, thus, reduce surface area and related capacity, i.e. product performance.

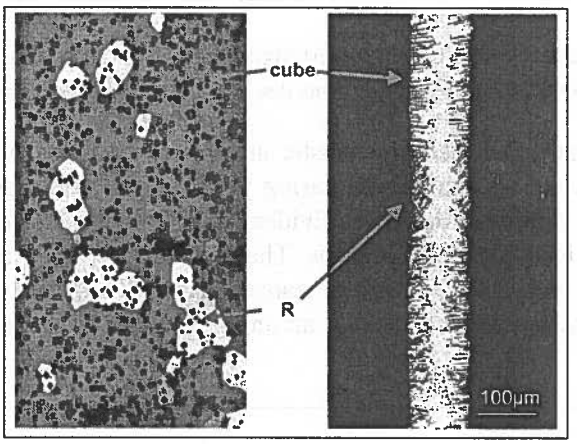

Fig. 12. High purity aluminum condenser foil with dominant cube and minor R texture (visualized by different etching techniques) and effects on surface by deep etching a) Barker etched surface: Dark areas and the quadratic etch pits indicate cube grains b) Longitudinal section of a "tunnel" deep etched condenser foil. Cube grains are etched vertical to the foil surface, increasing the efficient surface for high capacity

In order to achieve maximum cube texture in Al condenser foil of reduced thickness ($< 100\mu$m) in a technically feasible process, the initial hot rolling cube texture is of importance, which generates sufficient cube nucleation bands. Furthermore, special intermediate annealing treatments are needed to help the bands survive the severe large rolling deformation history [12, 20].

5. Summary and conclusions

The main textures observed in as cast, rolled and recrystallized aluminum alloys and their effect on strength, anisotropy and formability are described and related to variations in properties:

A $<100>$-fiber type is found in directionally solidified aluminum due to growth selection during solidification. It also occurs after uni-axial deformation, together with a dominant $<111>$ fiber due to selection of active slip systems. During plane strain deformation a corresponding rolling texture is formed. After subsequent recrystallization due to rolling at elevated temperatures or additional annealing of cold rolled sheet often a characteristic cube texture evolves. Under certain conditions also a randomization effect on texture can be observed by particle-stimulated nucleation (PSN). In any case recrystallization texture formation is controlled by the limited nucleation events and/or by a subsequent process of growth selection out of the corresponding orientation spectrum.

The principal effects on product properties are variations in:

a) Strength — either by the orientation dependence of slip or indirect by changing slip modes e.g. during age hardening.

b) Formability, where deformation geometry is affected e.g. in form of r-value in tensile deformation or cup height and flange thickness in deep drawing operations.

Since property control is a key issue in many practical applications textures and related process variables must be controlled accordingly. Furthermore, if clarified sufficiently quite useful information can be obtained about the underlying physical processes involved with the help of texture analysis of industrially processed material. These two aspects combine both the fundamental and the practical aspects of texture research for material control and process optimization in industrial application.

Acknowledgements

The author is grateful to Drs. O. Engler, J. Hasenclever and K. Karhausen for helpful discussions.

REFERENCES

[1] "Control of Directional Properties" edt. by H.J.Bunge, DGM- Informationsges. (1988).
[2] 'Numerical Predictions of Deformation Processes and the Behaviour of Real Materials' N.Hansen et.al. (eds.) 15th RISO International Symp., (1994).
[3] J. Hirsch, K. Karhausen, O. Engler, in "Continuum Scale Simulation of Engineering Materials" (edt. By D.Raabe et. Al.) 2004, Wiley-VCH, Weinheim, p.705-725
[4] "Experimental Techniques of Texture Analysis", ed. by H.J. Bunge, DGM-Oberursel (1985).
[5] B.J. Adams, S.I. soWright, K. Kunze, Metall Trans. **24A**, 819 (1993).
[6] V. Randle, O. Engler, "Introduction to Texture Analysis: Macrotexture, Microtexture and Orientation Mapping", Gordon and Breach, 2000.
[7] H.J. Bunge, "Mathematical Methods of Texture Analysis", Butterworths, London (1981).
[8] J. Hirsch, E. Nes, K. Lücke, Acta metall. **34**, 427-438 (1987).
[9] J. Hirsch, K. Lücke, Acta Metall. Overview No. 76, **36**, 11, 2863-2927 (1988).

[10] J. Hirsch, O. Engler.RexGG 1st joint int. Conference on Recrystallization and Grain Growth /Aachen edt. by G.Gottstein, D.Molodov, Springer Verlag Berlin **2**, 731-740 (2001).
[11] R.D. Doherty, Prog. Mater. Sci. **42**, 39-58. 1997.
[12] J. Hirsch, O. Engler, in "Microstructural and Crystallographic Aspects of Recrystallisation", 16th Risø Int. Symp. , ed. by N. Hansen et al., Risø Nat. Lab., Roskilde 49-62, Denmark 1995.
[13] O. Engler, J. Hirsch, Materials Science and Engineering A **336**, 249 (2002).
[14] J. Hirsch, P. Wagner, H. Schmiedel, Proc. ICAA-5 Mater. Sci. Forum, **217-222**, 641-646 (1996).
[15] G. Tempus, G. Scharf, W. Calles, Journal de Physique, 9, 48, *Proceedings* 4th Int. Conf. On Al-Li-Alloys, Paris (1987) C3-187.
[16] J. Hirsch, Material Science Forum **426**, edt. T.Chandra, Trans Tech Publications 185, Switzerland (2003).
[17] J. Hirsch, ASM- J.T.Staley Symp. Indianapolis, ed. by M.Tiryakioglu ASM-Int. Materials Park Ohio 276, (2001).
[18] B. Kernig, G. Scharf, R. Rixen, Z. Aluminium 65, 274 (1989).
[19] "Advances in Hot Deformation Textures and Microstructures", TMS/ASM symp. eds. J. Jonas, T. Bieler, K. Bowman, TMS, Warrendale PA, 1993.
[20] J. Hasenclever, G. Scharf, Proc. ICAA-5 Mater. Sci. Forum, **217-222**, 565-570 (1996).
[21] D. Raabe, K. Helmig, F. Roters, Z. Zhao, J. Hirsch, Materials Science Forum **408-412** 257. Transtec Publ., Switzerland (2002).

Received: 24 January 2005.